

A Global Infrasound Event Catalog

Abstract

The Comprehensive Nuclear Test Ban Treaty Organization is charged with generating automatic and manually reviewed global infrasound event catalogs for dissemination to national data centers. This is a challenging problem given the sparsity of International Monitoring System infrasound network, the time-varying atmospheric medium, and the large numbers of detections from local and coherent wave signals that can be falsely associated with detections at other arrays. By relying on a single algorithm, and without adequate ground-truth for assessment, it is difficult to estimate the missed detection rate. In this presentation, an independently generated global event catalog is presented that uses a completely different set of algorithms for infrasound event detection.

Method

Infrasound array detection is implemented using a parallel bank of detectors, which are combined following Fisher's method:

$$\chi^2 = -2 \sum_{i=1}^k \ln(p_i)$$

We currently combine detectors that are based on two different physical properties of long-range infrasound signals: (1) signal coherence, and (2) signal duration. Standard infrasound detectors are based on coherence; by adding a duration constraint we improve the detection of low-coherence signals (e.g., from multipathing) and avoid detecting short-duration local signals. Long-duration signals are found by identifying waveform segments with a small variance in backazimuth over a long time window. For both detectors, p-values are evaluated by describing the null hypothesis with an empirical model that is evaluated on real data using Kernel Density Estimation. No statistical assumptions are required. This p-value framework is completely general and allows for additional detectors for more targeted detection of specific event types.

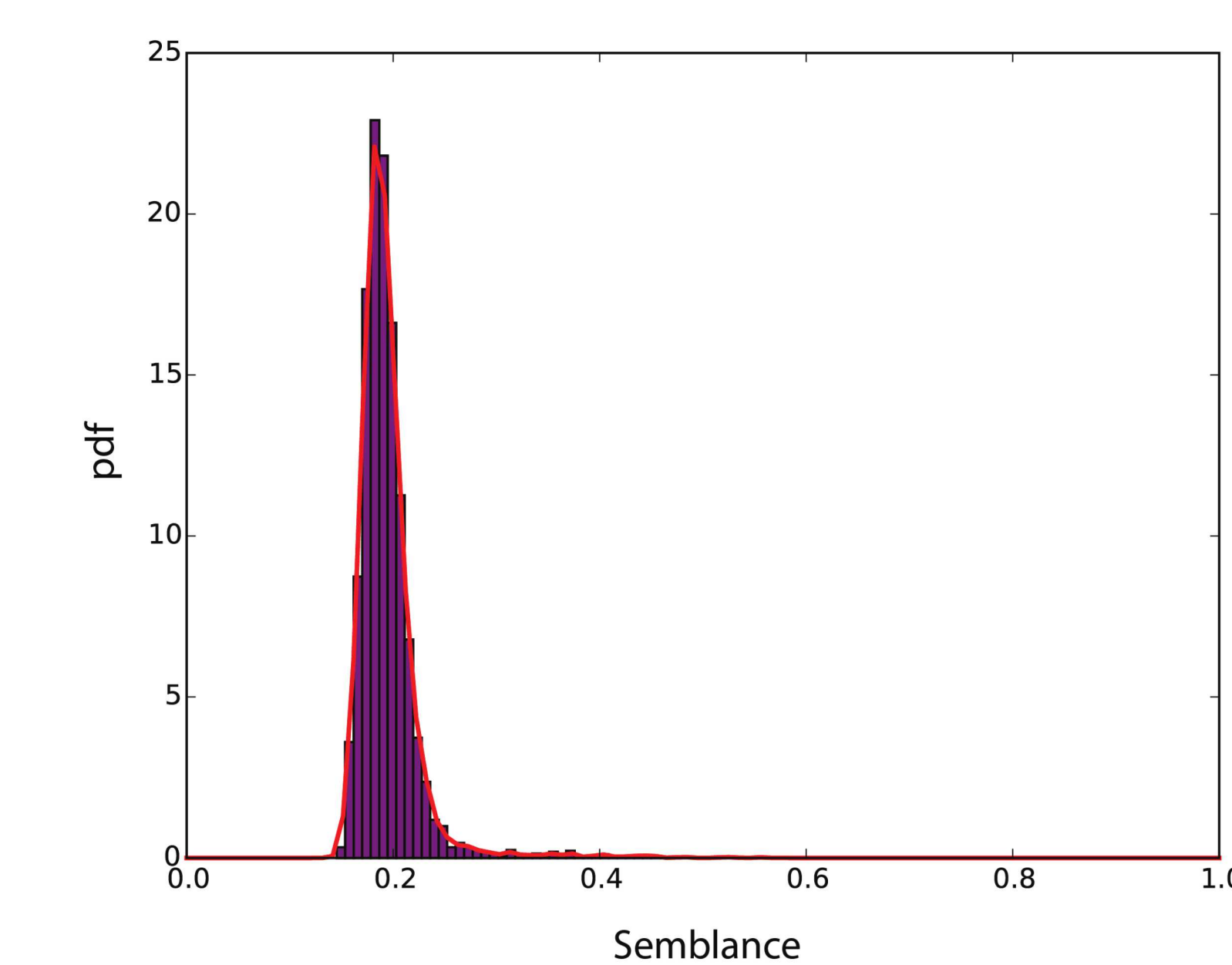


FIGURE 1. P-values are calculated by fitting the ambient distribution of each detection statistic (e.g., semblance, shown by the purple histogram) with a Kernel Density estimate (red curve). The use of a KDE ensures that tails are fit appropriately and that the distribution fit is not biased by the mode of the distribution.

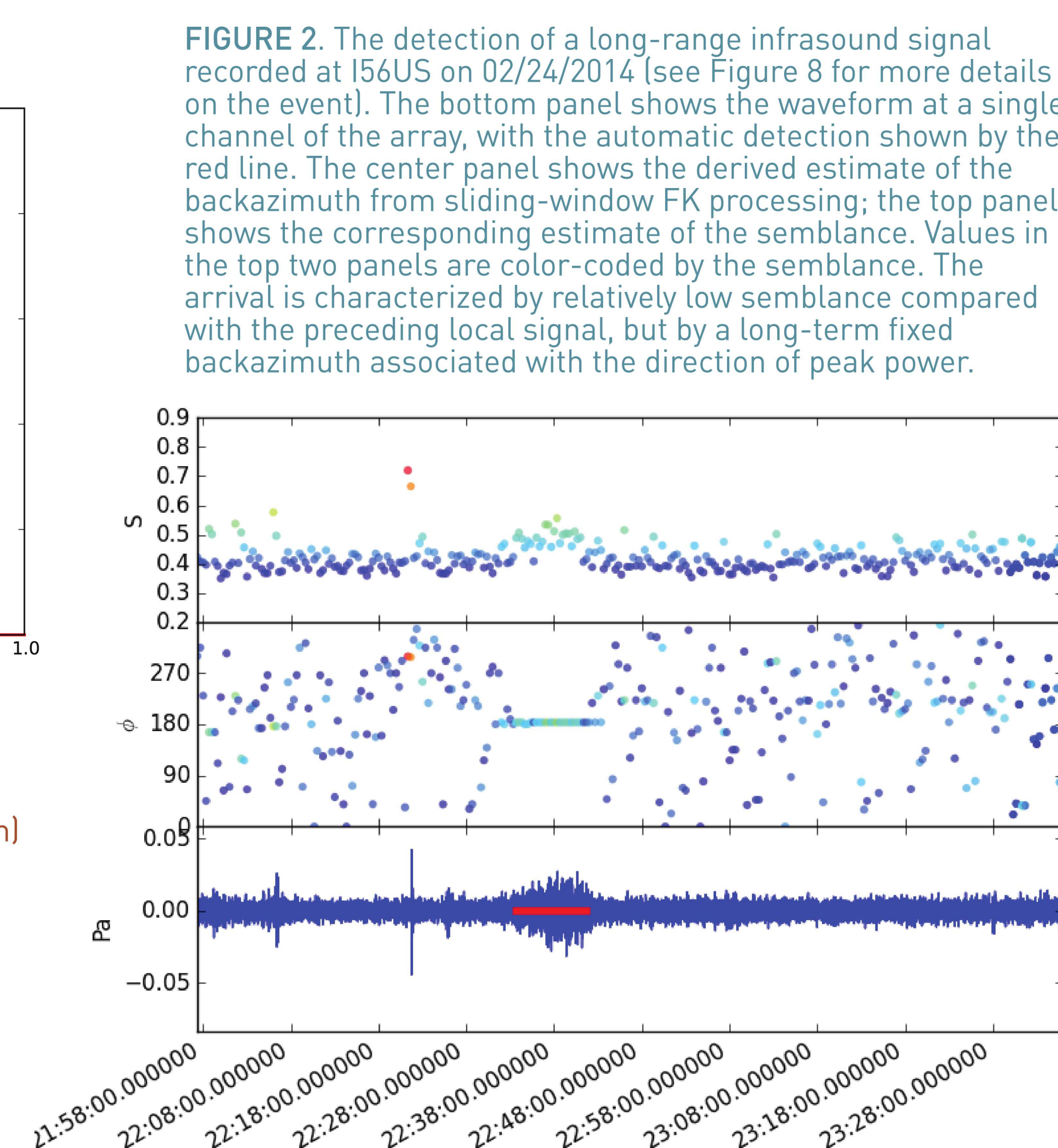


FIGURE 2. The detection of a long-range infrasound signal recorded at I56US on 02/24/2014 (see Figure 8 for more details on the event). The bottom panel shows the waveform at a single channel of the array, with the automatic detection shown by the red line. The center panel shows the derived estimate of the backazimuth from sliding-window FK processing; the top panel shows the corresponding estimate of the semblance. Values in the top two panels are color-coded by the semblance. The arrival is characterized by relatively low semblance compared with the preceding local signal, but by a long-term fixed backazimuth associated with the direction of peak power.

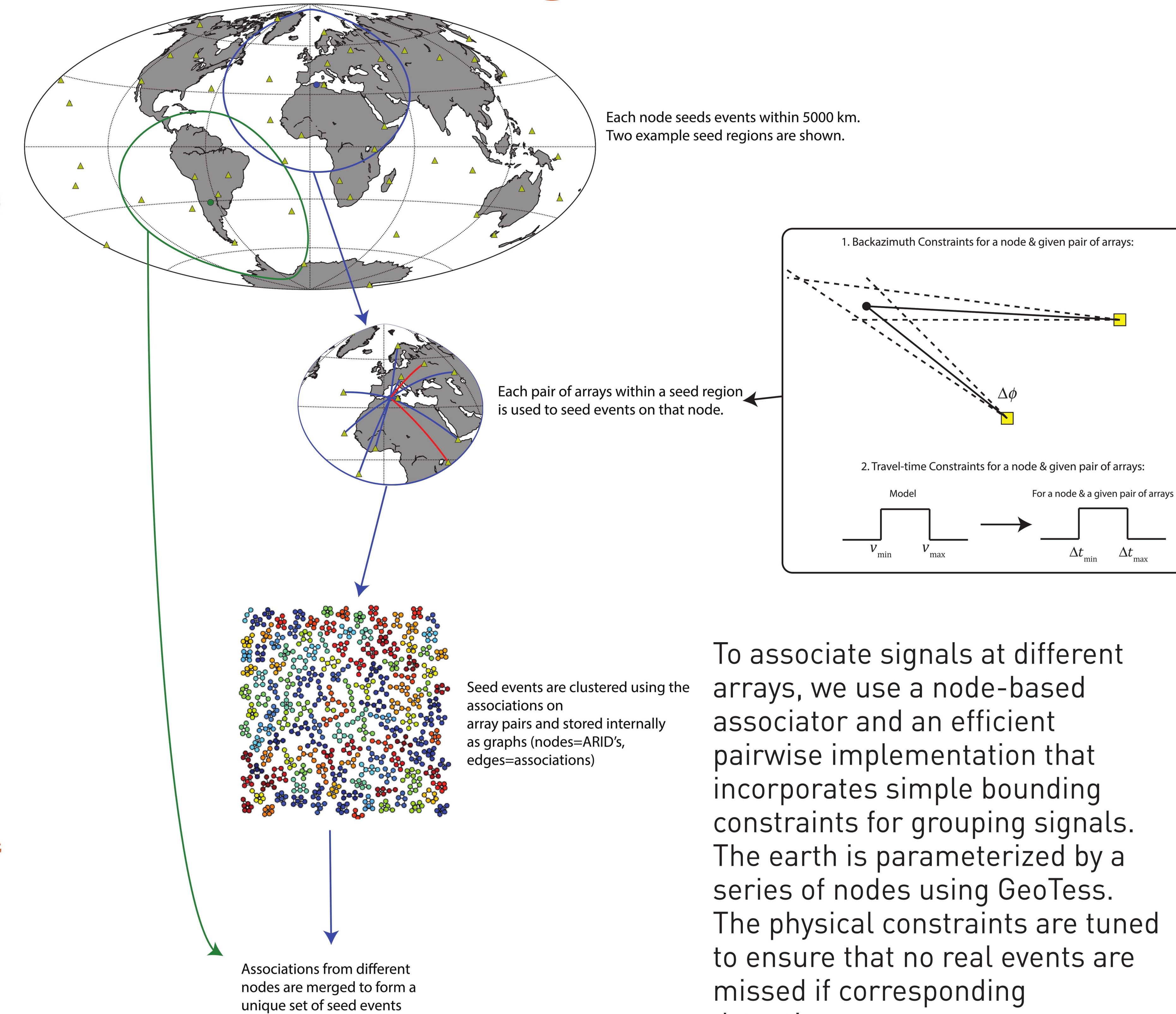


FIGURE 3. Illustration of the node-based association algorithm.

Dataset and Processing

Data have been processed from 47 arrays in the global IMS infrasound network in 2014 (Figure 4). Each array is first processed using standard sliding-window FK processing in two frequency bands: 0.01 - 0.5 Hz and 0.5 - 3 Hz. The filter bands are broadband compared with the data processing scheme used by the IDC. Next, the sliding-window FK results are processed using Fisher's method with both coherence and duration-based detectors to detect signals. The set of detections are processed using the node-based association scheme to identify events. On a 6-Core Intel Xeon E5 Mac Pro, the FK process takes ~3 days, detection process ~1 hour, and the association scheme ~3 hours to process 1-year of data on 47 arrays.



FIGURE 4. Data availability at SNL for the 47 arrays processed in this study.

Stephen J. Arrowsmith

Sandia National Laboratories

Results

The results obtained for the one-year period of study provide insights into the spatio-temporal variability of global coherent ambient infrasound, in addition to the global distribution of transient infrasound sources. Sliding-window FK processing results (e.g., Figure 5) highlights the effect of seasonal variations in the atmospheric state on the direction of coherent infrasound signals. By processing FK results at each array to find transient signals, the associated detection statistics (Figure 6) provide a preliminary assessment of the locations of transient infrasound events. Larger numbers of detections over the continents of the Northern Hemisphere are related to increased human activity in this region.

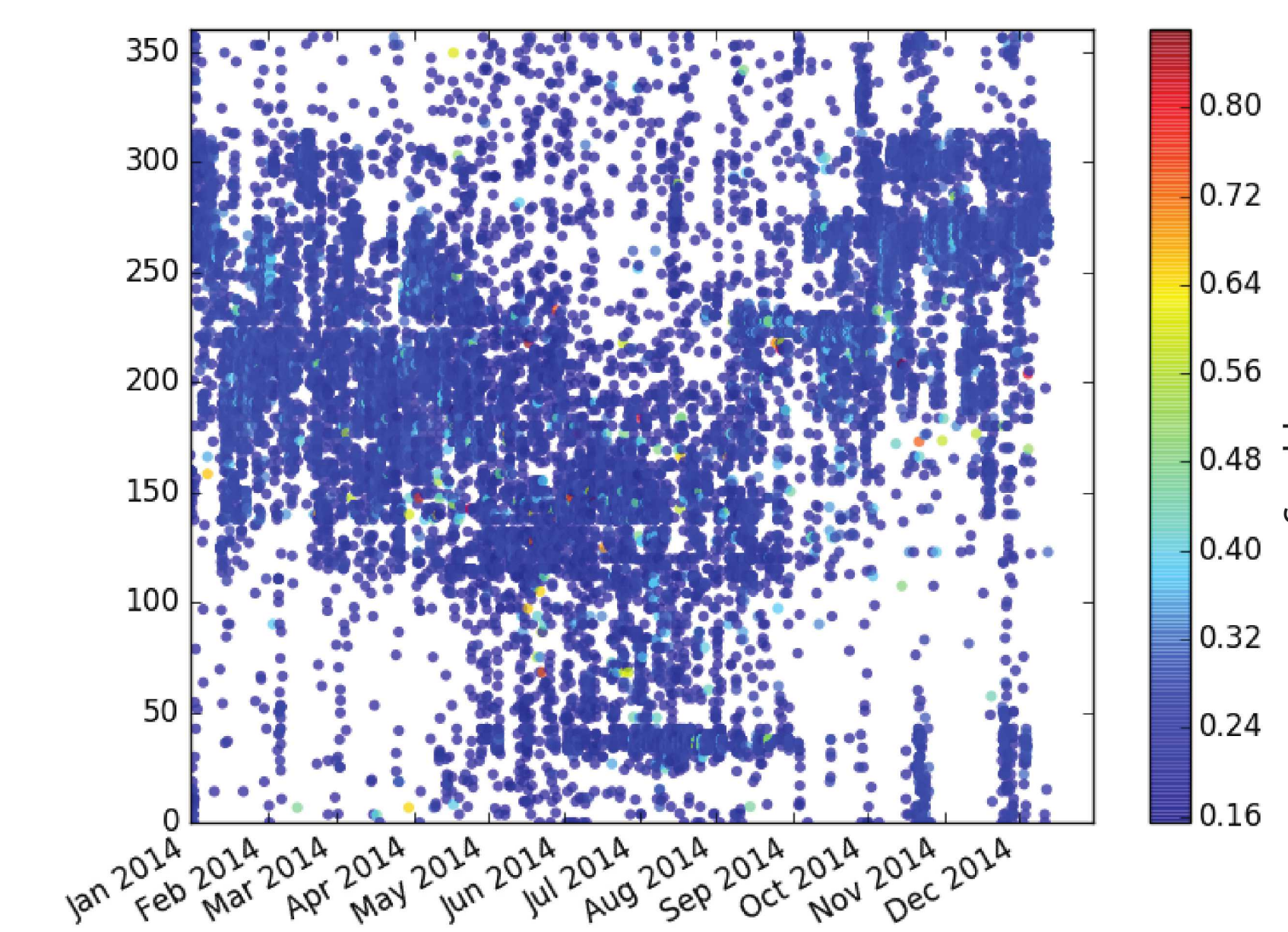


FIGURE 5. Temporal variation in the backazimuth of peak coherent infrasound in the 0.5 - 3 Hz band at I53US (Fairbanks, Alaska) as obtained from sliding-window FK processing. Long-period variations can be seen associated with seasonal changes in the stratospheric wind direction.

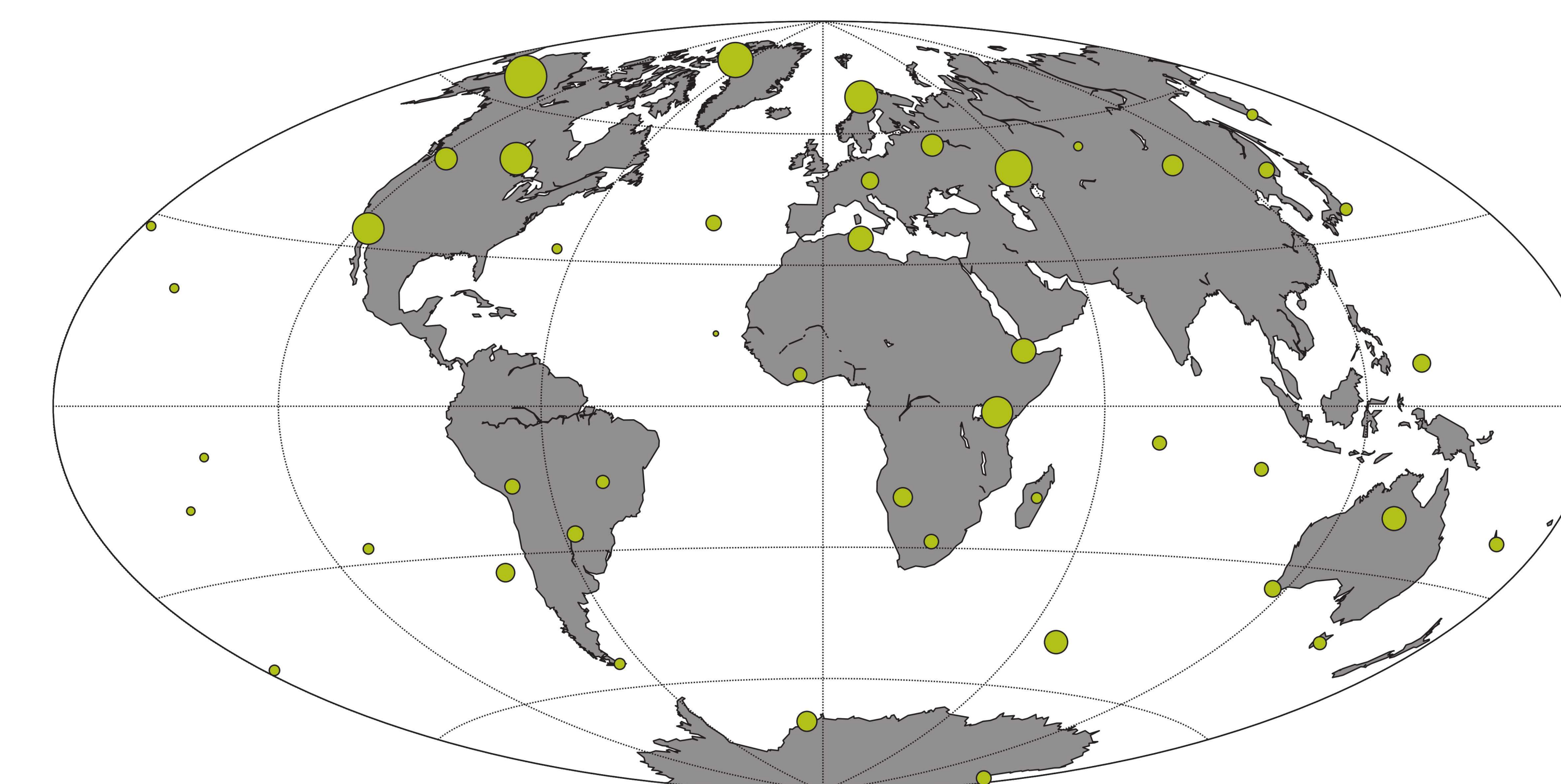


FIGURE 6. Number of detections obtained in the 1-year period at each of the 47 arrays in the IMS network (the numbers range from ~100 to ~10,000 in a one-year period). Larger numbers of detections are observed at continental arrays in the Northern Hemisphere, with fewer detections at oceanic arrays.

By processing the set of detections shown in Figure 6 with the node-based association algorithm, we obtain the event catalog shown in Figure 7. Clusters of events are found near the Black Sea, Fennoscandia, on the Arabian peninsula, in the Western US, Alaska, and over the North Atlantic Ocean. Many of these clusters are related to military and industrial activities. The relatively large cluster of events in the North Atlantic requires further investigation. Additional events that are detected include bolides and the eruption of Kelud volcano.

An example event is shown in Figure 8. This event occurs in a cluster of infrasound events that is related to military activity in the Western US.

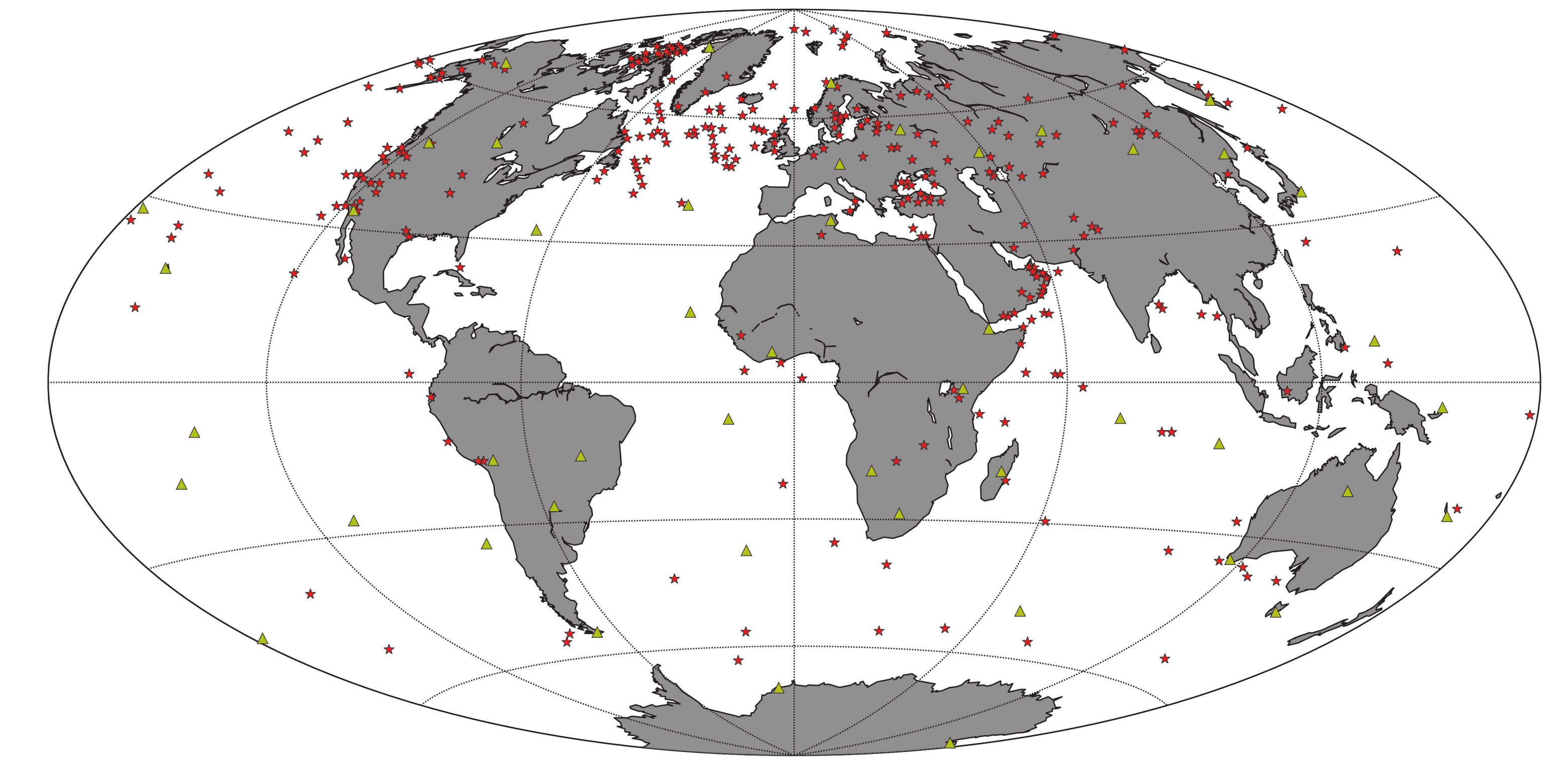


FIGURE 7. The global event catalog obtained for 2014 using the techniques described in this paper. Each red star denotes a separate event, with the location of each star denoting the node with the highest number of associations for that event (note that in some cases, multiple nodes have the same numbers of associating phases). Locations of the IMS infrasound arrays used in this study are shown by the yellow triangles.

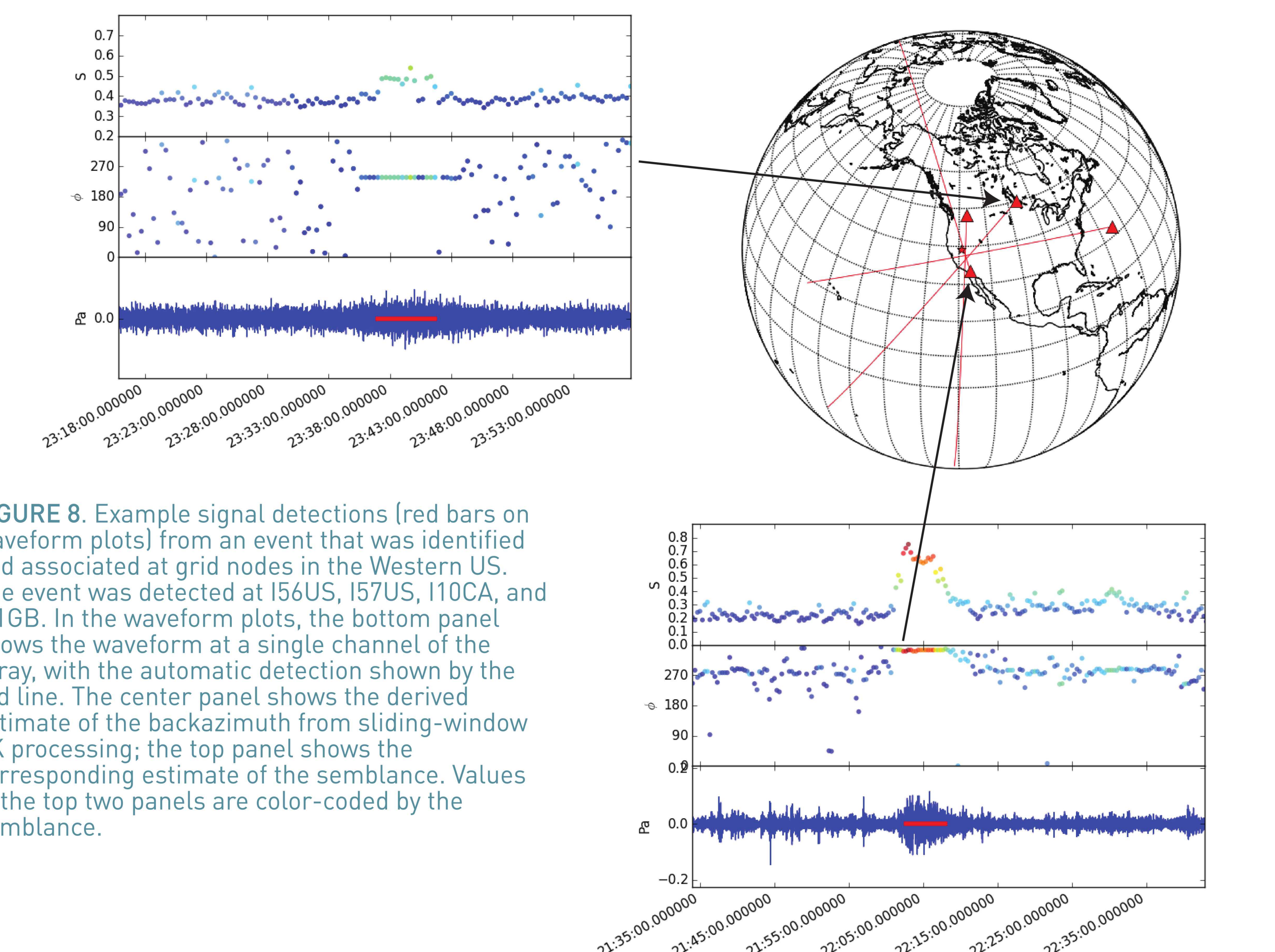


FIGURE 8. Example signal detections (red bars on waveform plots) from an event that was identified and associated at grid nodes in the Western US. The event was detected at I56US, I57US, I10CA, and I51GB. In the waveform plots, the bottom panel shows the waveform at a single channel of the array, with the automatic detection shown by the red line. The center panel shows the derived estimate of the backazimuth from sliding-window FK processing; the top panel shows the corresponding estimate of the semblance. Values in the top two panels are color-coded by the semblance.

Acknowledgements

The author is very grateful to Richard Stead at LANL for helping to backfill our infrasound holdings at SNL and to Dorthie Carr for support with the database at SNL. This work has benefited from discussions with Pierrick Mialle (CTBTO), David Green (AWE), and Dean Clauter (AFTAC).